

# Involvement of Inducible 6-Phosphofructo-2-kinase in the Anti-diabetic Effect of Peroxisome Proliferator-activated Receptor $\gamma$ Activation in Mice<sup>\*[5]</sup>

Received for publication, March 15, 2010, and in revised form, May 10, 2010. Published, JBC Papers in Press, May 24, 2010, DOI 10.1074/jbc.M110.123174

Xin Guo<sup>‡</sup>, Kefeng Xu<sup>§</sup>, Jifeng Zhang<sup>¶1</sup>, Honggui Li<sup>‡</sup>, Weiyu Zhang<sup>||</sup>, Huan Wang<sup>||</sup>, Alex J. Lange<sup>\*\*</sup>, Y. Eugene Chen<sup>¶1,2</sup>, Yuqing Huo<sup>||‡‡3</sup>, and Chaodong Wu<sup>‡4</sup>

From the <sup>‡</sup>Intercollegiate Faculty of Nutrition, Department of Nutrition and Food Science, Texas A&M University, College Station, Texas 77843, the <sup>§</sup>Cardiovascular Research Institute, Morehouse School of Medicine, Atlanta, Georgia 30310, the <sup>¶</sup>Cardiovascular Center, Department of Internal Medicine, University of Michigan Medical Center, Ann Arbor, Michigan 48105, the Departments of <sup>||</sup>Medicine and <sup>\*\*</sup>Biochemistry, Molecular Biology, and Biophysics, University of Minnesota Medical School, Minneapolis, Minnesota 55455, and the <sup>‡‡</sup>Institute of Molecular Medicine, Peking University, Beijing 100871, China

*PFKFB3* is the gene that codes for the inducible isoform of 6-phosphofructo-2-kinase (iPFK2), a key regulatory enzyme of glycolysis. As one of the targets of peroxisome proliferator-activated receptor  $\gamma$  (PPAR $\gamma$ ), PFKFB3/iPFK2 is up-regulated by thiazolidinediones. In the present study, using PFKFB3/iPFK2-disrupted mice, the role of PFKFB3/iPFK2 in the anti-diabetic effect of PPAR $\gamma$  activation was determined. In wild-type littermate mice, PPAR $\gamma$  activation (*i.e.* treatment with rosiglitazone) restored euglycemia and reversed high fat diet-induced insulin resistance and glucose intolerance. In contrast, PPAR $\gamma$  activation did not reduce high fat diet-induced hyperglycemia and failed to reverse insulin resistance and glucose intolerance in PFKFB3<sup>+/-</sup> mice. The lack of anti-diabetic effect in PFKFB3<sup>+/-</sup> mice was associated with the inability of PPAR $\gamma$  activation to suppress adipose tissue lipolysis and proinflammatory cytokine production, stimulate visceral fat accumulation, enhance adipose tissue insulin signaling, and appropriately regulate adipokine expression. Similarly, in cultured 3T3-L1 adipocytes, knockdown of PFKFB3/iPFK2 lessened the effect of PPAR $\gamma$  activation on stimulating lipid accumulation. Furthermore, PPAR $\gamma$  activation did not suppress inflammatory signaling in PFKFB3/iPFK2-knockdown adipocytes as it did in control adipocytes. Upon inhibition of excessive fatty acid oxidation in PFKFB3/iPFK2-knockdown adipocytes, PPAR $\gamma$  activation was able to significantly reverse inflammatory signaling and proinflammatory cytokine expression and restore insulin signaling. Together, these data demon-

strate that PFKFB3/iPFK2 is critically involved in the anti-diabetic effect of PPAR $\gamma$  activation.

Peroxisome proliferator-activated receptor  $\gamma$  (PPAR $\gamma$ )<sup>5</sup> is a nuclear receptor whose activation by thiazolidinediones (TZDs) effectively improves systemic insulin sensitivity and lowers plasma glucose levels in both human patients and rodent models of type 2 diabetes (1–8). Because TZDs are effective in liver- or muscle-specific PPAR $\gamma$ -deficient mice (9, 10) but not in adipose tissue-deleted mice (11) and adipose-specific PPAR $\gamma$ -deficient mice (12), adipose tissue has been considered as the primary target site for the anti-diabetic effect of PPAR $\gamma$  activation (13, 14). Further investigations have suggested two adipose tissue-based mechanisms to largely explain the anti-diabetic effect of PPAR $\gamma$  activation (6, 15). In the first mechanism, PPAR $\gamma$  activation by TZDs appropriately alters the expression of adipocyte genes that are involved in lipogenesis and triglyceride synthesis to increase the capacity of fat storage in adipose tissue (16–19). This leads to reduction of the circulating levels of free fatty acids (FFA) and thereby reversal of FFA-induced insulin resistance. In the second mechanism, PPAR $\gamma$  activation by TZDs suppresses the adipose tissue inflammatory response (20, 21) and appropriately regulates adipokine expression (6, 22, 23). This improves adipose tissue function, which in turn brings about the insulin-sensitizing effect (6). However, the molecular link between the two mechanisms remains to be elucidated.

Upon activation of PPAR $\gamma$ , a number of PPAR $\gamma$  target genes are altered to promote fat storage in adipose tissue (16, 24–26). For example, TZDs stimulate the expression of glycerol kinase (GyK), which increases triglyceride synthesis in adipocytes by providing glycerol 3-phosphate as a key substrate (16). Similarly, PPAR $\gamma$  activation stimulates the expression of the cyto-

\* This work was supported, in whole or in part, by National Institutes of Health Grants HL78679 and HL080569 (to Y. H.) and HL68878, HL89544, and HL75397 (to Y. E. C.). This work was also supported by American Diabetes Association Grants 1-10-B5-76 (to Y. H.) and 1-10-JF-54 (to C. W.).

[5] The on-line version of this article (available at <http://www.jbc.org>) contains supplemental Figs. S1 and S2.

<sup>1</sup> Supported by American Heart Association National Career Development Grant 0835237N.

<sup>2</sup> An established investigator of the American Heart Association (Grant 0840025N). To whom correspondence may be addressed: 1150 W. Medical Center Dr., MSRB III 7301E, Ann Arbor, MI 48105. Fax: 734-936-2641; E-mail: echenum@med.umich.edu.

<sup>3</sup> To whom correspondence may be addressed: 420 Delaware St. SE, MMC508, Minneapolis, MN 55455. Fax: 612-626-4411; E-mail: yuqing@umn.edu and Institute of Molecular Medicine, Peking University, Beijing 100871, China.

<sup>4</sup> To whom correspondence may be addressed: 2253 TAMU, College Station, TX 77843. Fax: 979-862-7782; E-mail: cdwu@tamu.edu.

<sup>5</sup> The abbreviations used are: PPAR $\gamma$ , peroxisome proliferator-activated receptor  $\gamma$ ; iPFK2, inducible 6-phosphofructo-2-kinase; F26P<sub>2</sub>, fructose-2,6-bisphosphate; TZD, thiazolidinedione; GyK, glycerol kinase; PEPCK, phosphoenolpyruvate carboxykinase; ROS, reactive oxygen species; JNK, c-Jun N-terminal kinase; NF- $\kappa$ B, nuclear factor  $\kappa$ B; TNF $\alpha$ , tumor necrosis factor  $\alpha$ ; IL-6, interleukin-6; FFA, free fatty acid(s); HFD, high fat diet; PBS, phosphate-buffered saline; KD, kinase-dead; Ctrl, control; RT, reverse transcription.

## Involvement of *i*PFK2 in the Effect of PPAR $\gamma$ Activation

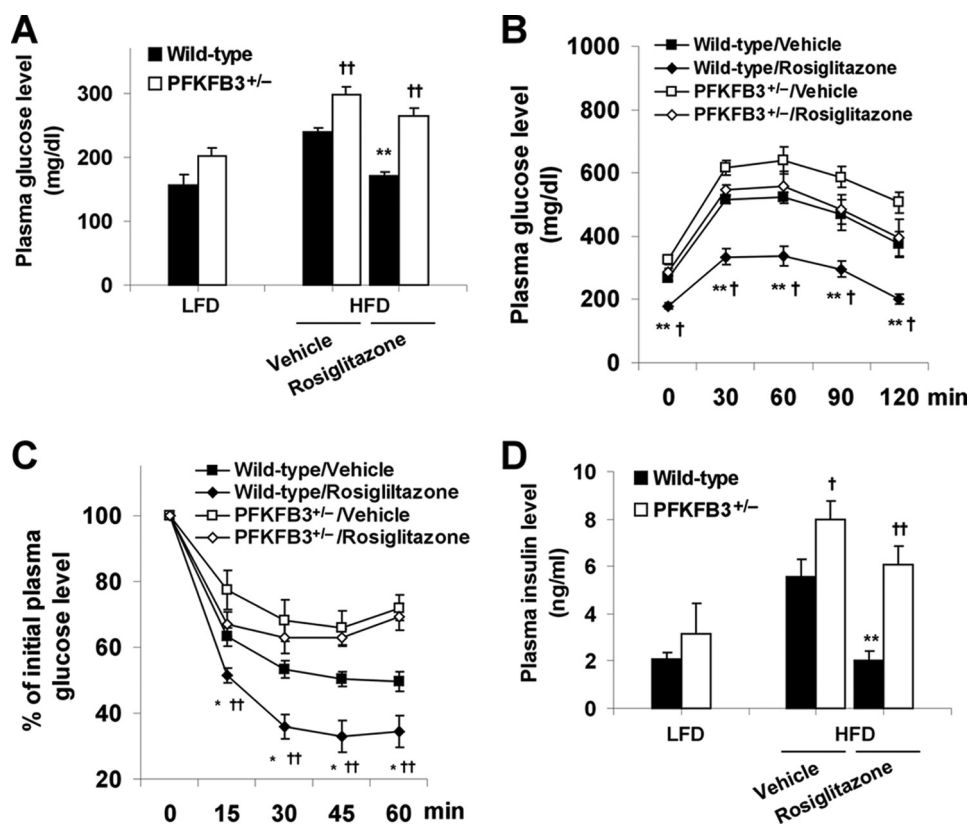


**FIGURE 1. Disruption of PFKFB3/iPFK2 blunts the anti-diabetic effect of PPAR $\gamma$  activation.** Male PFKFB3<sup>+/-</sup> mice and wild-type littermates, at the age of 5–6 weeks, were fed an HFD for 12 weeks and treated with rosiglitazone (10 mg/kg/day) or vehicle (PBS) during the last 4 weeks of HFD feeding. Data are means  $\pm$  S.E. (error bars),  $n = 6$ . **A**, changes in the levels of plasma glucose. As the control, the age-matched male PFKFB3<sup>+/-</sup> mice and wild-type littermates were fed a low fat diet (LFD) and received no treatment. All of the mice were fasted for 4 h before collection of blood samples. \*\*,  $p < 0.01$ , rosiglitazone versus vehicle within the same genotype. †,  $p < 0.05$ ; ††,  $p < 0.01$ , PFKFB3<sup>+/-</sup> versus wild type on an HFD with the same treatment (rosiglitazone or vehicle). For **B** and **C**, mice were fasted for 4 h and received an intraperitoneal injection of  $\alpha$ -glucose (2 g/kg) (**B**) or insulin (0.5 units/kg) (**C**). \*,  $p < 0.05$ ; \*\*,  $p < 0.01$ , wild type/rosiglitazone versus wild type/vehicle. †,  $p < 0.05$ ; ††,  $p < 0.01$ , PFKFB3<sup>+/-</sup>/rosiglitazone versus wild type/rosiglitazone. **B**, glucose tolerance test. **C**, insulin tolerance test. **D**, changes in the levels of plasma insulin. Mice were fed and/or treated as described in **A**. Statistical analyses were identical to those in **A**.

solic isoform of phosphoenolpyruvate carboxykinase (PEPCK) in adipocytes (24, 25). This increases glyceroneogenesis and provides another way to synthesize glycerol 3-phosphate and consequently triglycerides in adipocytes/adipose tissue (27, 28). At this point, although the stimulatory effect of PPAR $\gamma$  activation on GyK and PEPCK expression is increasingly documented, the involvement of GyK and/or PEPCK in the anti-diabetic effect of PPAR $\gamma$  activation requires further exploration (29, 30). Furthermore, there are no published data to address whether or not GyK and/or PEPCK are involved in the anti-inflammatory effect of PPAR $\gamma$  activation. In response to TZDs, the expression of several proinflammatory genes is decreased in the adipose tissue in both rodents and human patients with type 2 diabetes (18, 31). Further, PPAR $\gamma$  activation in both adipose tissue macrophages and adipocytes contributes to the suppression of the adipose tissue inflammatory response (21, 32). To date, mediators that are involved in the effect of PPAR $\gamma$  activation on adipocyte inflammatory response are largely unknown.

PFKFB3/iPFK2 is a target gene of PPAR $\gamma$  (33) and is stimulated by TZDs (34). The expression of PFKFB3/iPFK2 is at high levels in adipose tissue and at very low levels in the liver and skeletal muscle (34, 35). We have recently demonstrated a

pivotal role for PFKFB3/iPFK2 in regulating adipose tissue function and systemic insulin sensitivity (36). Mechanistically, PFKFB3/iPFK2 protects against fatty acid oxidation-associated reactive oxygen species (ROS) production, thereby reducing inflammatory signaling through JNK1 and NF- $\kappa$ B pathways to suppress adipocyte inflammatory response (36). However, the extent to which PFKFB3/iPFK2 participates in the *in vivo* effects of PPAR $\gamma$  activation is not known. Using PFKFB3/iPFK2-disrupted mice, the present study demonstrates that PFKFB3/iPFK2 is involved in the anti-diabetic effect of PPAR $\gamma$  activation, probably by increasing the ability of adipose tissue to store fat and by suppressing adipose tissue inflammatory response. In addition, the mechanisms underlying the involvement of PFKFB3/iPFK2 in the effects of PPAR $\gamma$  activation are explored in cultured 3T3-L1 adipocytes.

## EXPERIMENTAL PROCEDURES

**Animal Experiments**—Because homozygous disruption of PFKFB3/iPFK2 is embryonic lethal (35), PFKFB3<sup>+/-</sup> mice, provided by Drs. Telang and Chesney (University of Louisville), were generated as described previously (35) and used

for the present study. Considering that rosiglitazone lowers the levels of plasma glucose and improves systemic insulin sensitivity only in diabetic mice, male PFKFB3<sup>+/-</sup> and wild-type littermates (C57BL/6J background) were fed a high fat diet (HFD) prior to treatment with rosiglitazone. It has been recently shown that feeding an HFD to PFKFB3<sup>+/-</sup> mice exacerbates systemic insulin resistance and adipose tissue inflammatory response (36). Briefly, all mice were maintained as previously described (36). At the age of 5–6 weeks, mice were fed an HFD (60% fat calories, 20% protein calories, and 20 carbohydrate calories) (Research Diets, Inc., New Brunswick, NJ) for 12 weeks. During the last 4 weeks of the feeding regimen, HFD-fed mice were treated with rosiglitazone (10 mg/kg/day in PBS; Avandia tablets) or vehicle (PBS) via oral gavages. As the control, the age-matched male mice were fed a low fat diet (10% fat calories, 20% protein calories, and 70% carbohydrate calories) and received no treatment. The composition of both HFD and low fat diet has been described previously (36). Body weight and food intake of the mice were recorded every 4 days during the 12-week feeding period. At the end of the feeding/treatment regimen, mice were fasted for 4 h before sacrifice for collection of blood and

tissue samples as described previously (36–39). Visceral fat content was estimated as the sum of epididymal, mesenteric, and perinephric fat depots (36, 38). After weighing, lipolysis rates were determined on adipose tissue samples. Some tissue samples were either fixed and embedded for histological analyses or frozen in liquid nitrogen and then stored at  $-80^{\circ}\text{C}$  for further analyses. Some mice were fasted similarly

**TABLE 1**
**General metabolic characteristics**

At the age of 5–6 weeks, male PFKFB3<sup>+/-</sup> mice and wild-type littermates were fed an HFD for 12 weeks. During the last 4 weeks of the HFD feeding regimen, mice were treated with rosiglitazone (10 mg/kg/day in PBS) or vehicle (PBS). Data are means  $\pm$  S.E.,  $n = 6$ . TG, triglycerides.

	Wild type		PFKFB3 <sup>+/-</sup>	
	Vehicle	Rosiglitazone	Vehicle	Rosiglitazone
<b>Body weight (g)<sup>a</sup></b>				
Prior to treatment	42.7 $\pm$ 1.2	43.7 $\pm$ 0.8	36.4 $\pm$ 1.0 <sup>b</sup>	36.8 $\pm$ 0.9 <sup>b</sup>
Post treatment	43.4 $\pm$ 1.3	46.9 $\pm$ 1.0 <sup>c,d</sup>	36.7 $\pm$ 1.0 <sup>b</sup>	37.3 $\pm$ 1.0 <sup>b</sup>
<b>Food intake (g/day)</b>	1.9 $\pm$ 0.1	2.1 $\pm$ 0.2	2.0 $\pm$ 0.1	2.0 $\pm$ 0.1
<b>Plasma parameters</b>				
FFA (mM)	0.2 $\pm$ 0.03	0.1 $\pm$ 0.02 <sup>c</sup>	0.3 $\pm$ 0.02 <sup>b</sup>	0.3 $\pm$ 0.04 <sup>b</sup>
TG (mg/dl)	48 $\pm$ 3	41 $\pm$ 1 <sup>c</sup>	52 $\pm$ 2	53 $\pm$ 6 <sup>b</sup>
Leptin (ng/dl)	62 $\pm$ 4	79 $\pm$ 1 <sup>c</sup>	43 $\pm$ 4 <sup>b</sup>	37 $\pm$ 4 <sup>b</sup>

<sup>a</sup> Body weight of the mice was recorded before and 4 weeks after treatment with rosiglitazone or vehicle.

<sup>b</sup>  $p < 0.05$  PFKFB3<sup>+/-</sup> vs. wild-type with the same treatment (rosiglitazone or vehicle).

<sup>c</sup>  $p < 0.05$  rosiglitazone versus vehicle for the same genotype.

<sup>d</sup>  $p < 0.05$  post-treatment versus prior to treatment (rosiglitazone).

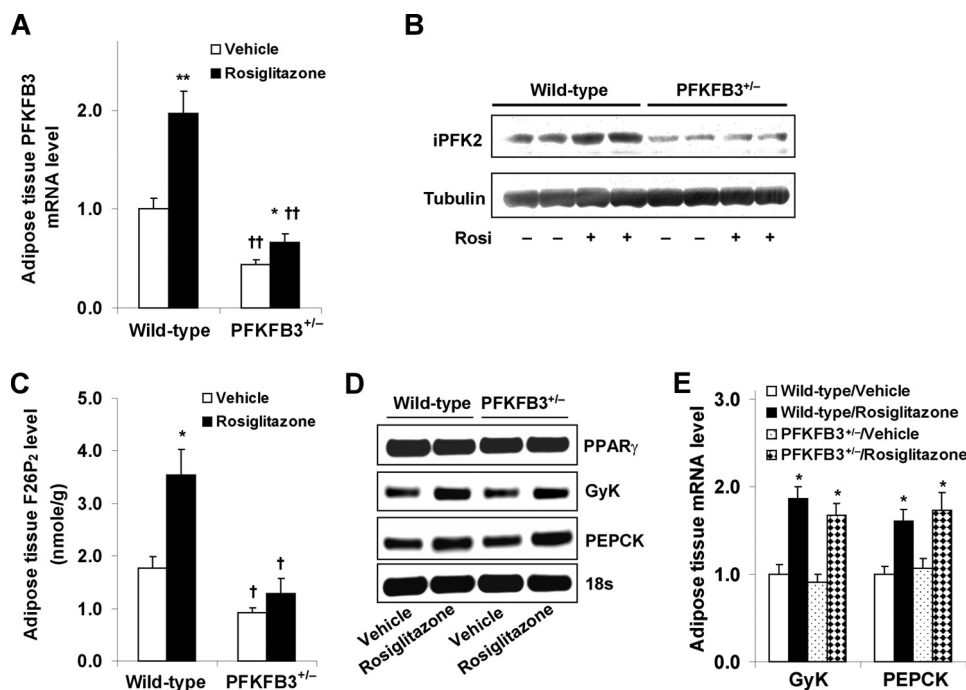


**FIGURE 2. Disruption of PFKFB3/*i*PFK2 impairs the response of adipose tissue PFKFB3 but not other PPAR $\gamma$  target genes to PPAR $\gamma$  activation.** At the age of 5–6 weeks, male PFKFB3<sup>+/-</sup> mice and wild-type littermates were fed an HFD for 12 weeks and treated with rosiglitazone (10 mg/kg/day) or vehicle (PBS) during the last 4 weeks of HFD feeding. At the end of the feeding/treatment regimen, mice were fasted for 4 h before collection of tissue samples. Epididymal adipose tissue samples were used for the analyses. *A*, the mRNA levels of PFKFB3 were measured using real-time RT-PCR. *B*, adipose tissue *i*PFK2 was determined using Western blot. *C*, adipose tissue F26P<sub>2</sub> levels were determined using the 6-phosphofructo-1-kinase activation method. *D*, representative PCR products of adipose tissue genes. *E*, quantification of the expression of adipose tissue genes. *Rosi*, rosiglitazone. For *A*, *C*, and *E*, data are means  $\pm$  S.E. (error bars),  $n = 6$ . \*,  $p < 0.05$ ; \*\*,  $p < 0.01$ , rosiglitazone versus vehicle within the same genotype (in *A* and *C*) or wild type/rosiglitazone versus wild type/vehicle and PFKFB3<sup>+/-</sup>/rosiglitazone versus PFKFB3<sup>+/-</sup>/vehicle for the same gene (in *E*). †,  $p < 0.05$ ; ††,  $p < 0.01$ , PFKFB3<sup>+/-</sup> versus wild type with the same treatment (rosiglitazone or vehicle in *A* and *C*).

and used for glucose and insulin tolerance tests. For a separate study to analyze the role of PPAR $\gamma$  in regulating PFKFB3 expression, PPAR $\gamma$ 2<sup>-/-</sup> mice and their wild-type littermates were generated as described before (40) and used for adipose tissue sample collection and embryonic fibroblast isolation (see below). All study protocols were reviewed and approved by the Institutional Animal Care and Use Committees of Texas A&M University and the University of Michigan.

**Measurement of Metabolite and Hormone Levels**—The levels of plasma metabolites, such as glucose, triglycerides, and FFA, were measured using metabolic assay kits (Sigma and BioVision (Mountain View, CA)). The levels of plasma hormones (*i.e.* insulin and leptin) were measured using enzyme-linked immunosorbent assay kits (Crystal Chem Inc., Downers Grove, IL). The levels of adipose tissue fructose 2,6-bisphosphate (F26P<sub>2</sub>) were determined using the 6-phosphofructo-1-kinase activation method as described previously (39).

**Glucose and Insulin Tolerance Tests**—The assays were conducted as previously described (39). After fasting for 4 h, mice received a peritoneal injection of D-glucose (2 g/kg) or insulin (0.5 unit/kg) (Humulin®, Lilly).

**Measurement of Adipose Tissue Lipolysis**—The assays were conducted as described previously (36, 41, 42). Briefly, freshly isolated adipose tissue samples were washed several times with PBS and incubated in a final volume of 1 ml of high glucose Dulbecco's modified Eagle's medium containing 2% fatty acid-free bovine serum albumin in the presence or absence of 10  $\mu\text{M}$  isoproterenol at 37  $^{\circ}\text{C}$  for 3 h. Aliquots of the medium were sampled hourly to quantify glycerol content using metabolic kits (BioVision, Mountain View, CA). The rate of lipolysis was estimated as the efflux of glycerol.

**Histological Analyses of Adipose Tissue**—The paraffin-embedded adipose tissue blocks were cut into sections of 5- $\mu\text{m}$  thickness and stained with hematoxylin and eosin.

**Cell Culture and Treatment**—3T3-L1 cells were maintained in high glucose Dulbecco's modified Eagle's medium and differentiated in induction medium for 6–8 days as described previously (36). To clarify the role of PPAR $\gamma$  activation in stimulating PFKFB3 expression, differentiated 3T3-L1 cells were treated with a PPAR $\alpha$  agonist, Wy14643 (10  $\mu\text{M}$ ) or GW7647 (0.1  $\mu\text{M}$ ); a dual agonist of PPAR $\alpha$  and PPAR $\delta$ , GW0742 (0.2  $\mu\text{M}$ ); a PPAR $\delta$  agonist, GW501516 (0.2  $\mu\text{M}$ ); a PPAR $\gamma$  agonist, GW7845 (0.2  $\mu\text{M}$ ) or rosiglitazone (1  $\mu\text{M}$ ); or vehicle (0.1% DMSO) for 24 h and har-

## Involvement of *i*PFK2 in the Effect of PPAR $\gamma$ Activation

vested for further analyses. In addition, mouse embryonic fibroblast cells were isolated from PPAR $\gamma$ <sup>2+/+</sup> mice and PPAR $\gamma$ <sup>2-/-</sup> mice and treated with retrovirus containing the cDNA of PPAR $\gamma$ 1, PPAR $\gamma$ 2, or control as described previously (40). The treated mouse embryonic fibroblast cells were then harvested to determine changes in the mRNA levels of PFKFB3. Using a PFKFB3 promoter-luciferase construct, the effect of PPAR $\gamma$ 2 overexpression on activating PFKFB3 promoter was determined by the luciferase assay as described by Cao *et al.* (43). To explore the direct role of PFKFB3/*i*PFK2 in modulating the effect of PPAR $\gamma$  activation, stable PFKFB3/*i*PFK2-knockdown (*i*PFK2-KD) 3T3-L1 cells and control (*i*PFK2-Ctrl) 3T3-L1 cells were used. These cells have been previously established (36). During the last 48 h of differentiation, both *i*PFK2-KD and *i*PFK2-Ctrl adipocytes were treated with rosiglitazone (1  $\mu$ M) or vehicle (0.1% DMSO) and used to quantify the expression of PPAR $\gamma$  target genes as well as for further analyses using the methods described below.

To quantify adipocyte lipid content, the cells were stained with Oil Red O. The lipid-associated dye was extracted with isopropyl alcohol for 15 min. The OD of the extraction solution was measured using a spectrophotometer at 510 nm (40). To determine the rate of glucose incorporation into lipid, each well (6-well plate) of the cells was incubated with Dulbecco's modified Eagle's medium supplemented with 1  $\mu$ Ci of [U-<sup>14</sup>C]glucose for 24 h as described previously (44). After sequential extraction with 30% KOH, 95% ethanol, 9 M H<sub>2</sub>SO<sub>4</sub>, and petroleum ether, the amount of <sup>14</sup>C-labeled lipids was quantified using a Beckman liquid scintillation counter. To analyze inflammatory signaling, the cells were incubated with palmitate (250  $\mu$ M) or vehicle (0.5% bovine serum albumin) for 24 h. Cell lysates were then prepared and used for Western blots to measure the levels and phosphorylation states of JNK and NF- $\kappa$ B p65. To determine adipocyte expression of proinflammatory cytokines and adipokines, the total RNA of the cells was prepared and used for real-time RT-PCR. To determine changes in insulin signaling, the cells were treated with or without insulin (100 nM) for 30 min prior to harvest. Cell lysates were prepared and used to measure the levels and phosphorylation of Akt using Western blots.

PFKFB3/*i*PFK2-knockdown-associated increase in fatty acid oxidation triggers adipocyte inflammatory response (36), which may account for lessening or blunting of the anti-inflammatory effect of PPAR $\gamma$  activation. To verify this concept, the differentiated stable *i*PFK2-KD and *i*PFK2-Ctrl adipocytes were treated with rosiglitazone (1  $\mu$ M) or vehicle (0.1% DMSO) for 48 h. In the last 24 h, 100  $\mu$ M etomoxir (an inhibitor of carnitine palmitoyltransferase-1), with or without palmitate (250  $\mu$ M), was added to rosiglitazone-treated cells. Thereafter, the cells were used to measure the production of ROS using the nitro blue tetrazolium assay as described previously (45) or harvested to analyze adipocyte inflammatory response and insulin signaling as described above.

**RNA Isolation, Reverse Transcription, and Real-time PCR**—The total RNA was isolated from frozen tissue samples and cultured cells. RNA isolation and real-time RT-PCR were conducted as described previously (36, 39). The mRNA levels were analyzed for PFKFB3, GyK, PEPCK, PPAR $\gamma$ , resistin, adiponec-

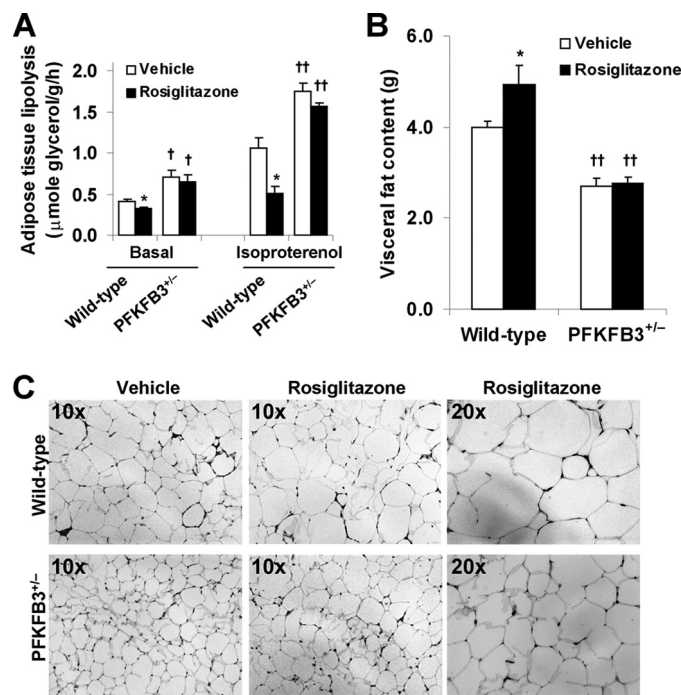


**FIGURE 3. Disruption of PFKFB3/*i*PFK2 lessens the effect of PPAR $\gamma$  activation on increasing adipose tissue fat storage.** At the age of 5–6 weeks, male PFKFB3<sup>+/-</sup> mice and wild-type littermates were fed an HFD for 12 weeks and treated with rosiglitazone (10 mg/kg/day) or vehicle (PBS) during the last 4 weeks of HFD feeding. At the end of the feeding/treatment regimen, mice were fasted for 4 h before collection of tissue samples. For A and B, data are means  $\pm$  S.E. (error bars),  $n = 6$ . \*,  $p < 0.05$  rosiglitazone versus vehicle within the same genotype (in A and B) in the presence of the same condition (in A, basal or isoproterenol). †,  $p < 0.05$ ; ††,  $p < 0.01$ , PFKFB3<sup>+/-</sup> versus wild type with the same treatment (in A and B, rosiglitazone or vehicle) in the presence of the same condition (in A, basal or isoproterenol). A, the rates of adipose tissue lipolysis were measured under both basal and isoproterenol-stimulated conditions. B, visceral fat content was estimated from the sum of epididymal, mesenteric, and perinephric fat mass. C, adipose tissue histology. The sections of epididymal fat pad were stained with hematoxylin and eosin.

tin, tumor necrosis factor  $\alpha$  (TNF $\alpha$ ), and interleukin-6 (IL-6) in adipose tissue samples and/or cell samples.

**Western Blots**—Lysates were prepared from frozen tissue samples and cultured cells. Western blots were conducted as described previously (38, 39). The levels of JNK, phospho-JNK, NF- $\kappa$ B p65, phospho-p65, Akt1/2, and phospho-Akt (Ser<sup>473</sup>) were analyzed.

**Statistical Methods**—Numeric data are presented as means  $\pm$  S.E. Statistical significance was assessed by unpaired, two-tailed analysis of variance or Student's *t* test. Differences were considered significant at the two-tailed  $p < 0.05$ .

## RESULTS

**Disruption of PFKFB3/*i*PFK2 Blunts the Anti-diabetic Effect of PPAR $\gamma$  Activation**—After a feeding of an HFD, wild-type littermates exhibited insulin resistance, glucose intolerance, and hyperglycemia. In these wild-type mice, treatment with rosiglitazone for 4 weeks normalized the levels of plasma glucose (169.67  $\pm$  6.05 versus 242.59  $\pm$  6.23 mg/dl,  $p < 0.01$ ; Fig. 1A) and corrected glucose intolerance and insulin resistance (Fig. 1, B and C) compared with vehicle. Additionally, treatment with rosiglitazone lowered the circulating levels of insulin (Fig. 1D) as well as FFA and triglycerides (Table 1), indicating the

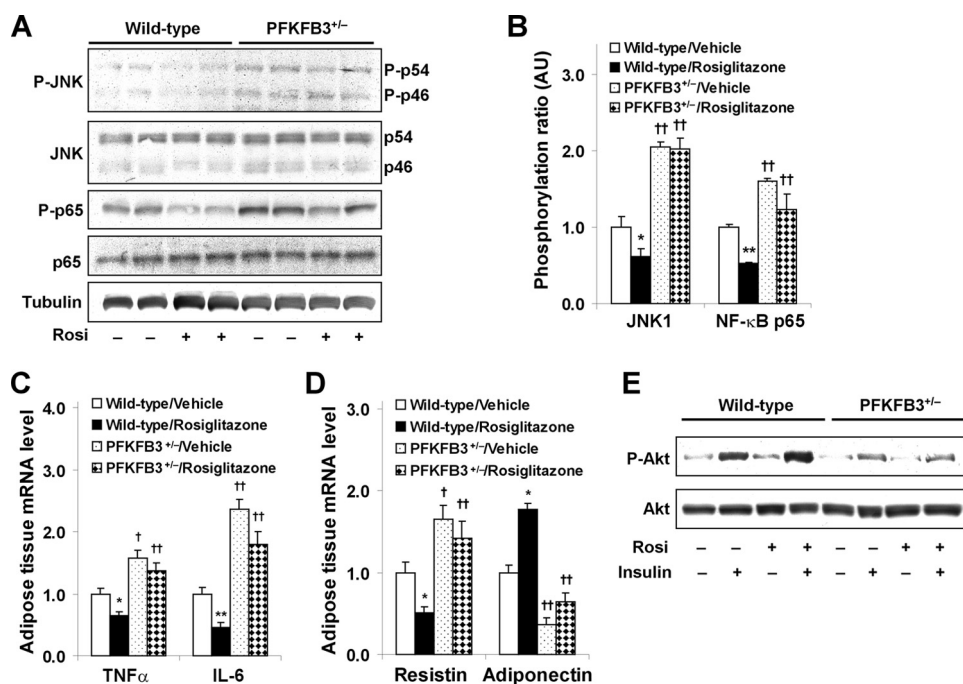


**FIGURE 4. Disruption of PFKFB3/iPFK2 blunts the effects of PPAR $\gamma$  activation on suppression of HFD-induced adipose tissue inflammatory response and on reversal of adipose tissue dysfunction.** At the age of 5–6 weeks, male PFKFB3 $^{+/-}$  mice and wild-type littermates were fed an HFD for 12 weeks and treated with rosiglitazone (10 mg/kg/day) or vehicle (PBS) during the last 4 weeks of HFD feeding. At the end of the feeding/treatment regimen, mice were fasted for 4 h before the collection of tissue samples. *Rosi*, rosiglitazone. **A**, changes in inflammatory signaling were analyzed using Western blots. **B**, quantification of inflammatory signaling (arbitrary units). **C**, changes in adipose mRNA levels of TNF $\alpha$  and IL-6. **D**, changes in adipose mRNA levels of resistin and adiponectin. For **B** and **D**, data are means  $\pm$  S.E. (error bars),  $n = 6$ . \*,  $p < 0.05$ ; \*\*,  $p < 0.01$ , wild type/rosiglitazone versus wild type/vehicle for the same gene. †,  $p < 0.05$ ; ††,  $p < 0.01$  PFKFB3 $^{+/-}$ /vehicle versus wild type/vehicle or PFKFB3 $^{+/-}$ /rosiglitazone versus wild type/rosiglitazone for the same gene. For **C** and **D**, the expression of adipose tissue genes was measured using real-time RT-PCR. **E**, adipose tissue insulin signaling was analyzed using Western blot. Adipose tissue samples were collected at 5 min after a bolus injection of insulin (1 unit/kg) into the portal vein. P-p54, phospho-p54; P-p46, phospho-p46; P-Akt, phospho-Akt.

reversal of hyperinsulinemia and hyperlipidemia. These data confirmed the anti-diabetic effect of PPAR $\gamma$  activation. Consistent with our previous study (36), feeding an HFD to PFKFB3 $^{+/-}$  mice exacerbated systemic insulin resistance and adipose tissue inflammatory response. In these PFKFB3/iPFK2-disrupted mice, treatment with rosiglitazone only caused an insignificant decrease in the levels of plasma glucose ( $263.14 \pm 13.20$  versus  $297.05 \pm 12.30$  mg/dl; Fig. 1A) and failed to improve insulin resistance and glucose intolerance. Thus, disruption of PFKFB3/iPFK2 blunts the anti-diabetic effect of PPAR $\gamma$  activation.

*Disruption of PFKFB3/iPFK2 Impairs the Response of Adipose Tissue PFKFB3/iPFK2 but Not Other PPAR $\gamma$  Target Genes to PPAR $\gamma$  Activation*—TZDs primarily target adipose tissue (11, 12) and stimulate the expression of PFKFB3/iPFK2 in adipocytes (34). In response to treatments with various PPAR activators, PFKFB3/iPFK2 in 3T3-L1 adipocytes was increased in a PPAR $\gamma$  activation-specific manner (supplemental Fig. S1A). Additionally, PPAR $\gamma$ 2 appears to mediate most of the effects of PPAR $\gamma$  activation on stimulating PFKFB3/iPFK2 (supplemental Fig. S1, B–D). To address the link between adipose tissue PFKFB3/iPFK2 and the anti-diabetic effect of PPAR $\gamma$  activation, the response of adipose tissue PFKFB3/iPFK2 to rosiglitazone was determined. Compared with vehicle, rosiglitazone treatment caused a significant increase in the mRNA

levels of adipose PFKFB3/iPFK2 in wild-type littermates, confirming the stimulatory effect of PPAR $\gamma$  activation. However, this stimulatory effect was markedly lessened in PFKFB3 $^{+/-}$  mice (Fig. 2, A and B). Because PFKFB3/iPFK2 determines the production of F26P $_2$ , the levels of adipose tissue F26P $_2$  were quantified to reflect PFKFB3/iPFK2 activity. Consistent with an increase in the mRNA levels of PFKFB3/iPFK2, the levels of adipose tissue F26P $_2$  were significantly higher in rosiglitazone-treated wild-type mice ( $3.54 \pm 0.48$  versus  $1.77 \pm 0.21$  nmol/g,  $p < 0.05$ ; Fig. 2C). However, in PFKFB3 $^{+/-}$  mice, rosiglitazone only caused a slight and insignificant increase in the levels of F26P $_2$  compared with vehicle ( $1.29 \pm 0.29$  versus  $0.92 \pm 0.08$  nmol/g). These data suggest that two intact PFKFB3/iPFK2 alleles are necessary for mice to fully respond to PPAR $\gamma$  activation.

To address whether disruption of PFKFB3/iPFK2 impairs the response of other PPAR $\gamma$  target genes to PPAR $\gamma$  activation, the expression of GyK and PEPCK as well as PPAR $\gamma$  in the adipose tissue was

determined. Under the basal condition (treatment with vehicle), the expression of the GyK, PEPCK, and PPAR $\gamma$  in PFKFB3 $^{+/-}$  mice did not differ from that in wild-type mice (Fig. 2, D and E). Furthermore, in response to PPAR $\gamma$  activation by rosiglitazone treatment, the expression of GyK and PEPCK in PFKFB3 $^{+/-}$  mice was increased to an extent comparable with that in wild-type littermates (Fig. 2, D and E). These data indicate that PPAR $\gamma$  expression, PPAR $\gamma$  translocation to cell nuclei, and activation of PPAR $\gamma$ -targeted genes are not disturbed in PFKFB3 $^{+/-}$  mice.

*Disruption of PFKFB3/iPFK2 Lessens the Effect of PPAR $\gamma$  Activation on Increasing Adipose Tissue Fat Storage*—Increasing adipose tissue fat storage, to a large extent, accounts for the anti-diabetic and insulin-sensitizing effects of PPAR $\gamma$  activation (16, 18, 26). In the present study, changes in the levels of plasma FFA and triglycerides as well as the rate of adipose tissue lipolysis, the content of visceral fat, and the size of epididymal adipocytes were determined to address the extent to which PPAR $\gamma$  activation increases the ability of adipose tissue to store fat in the mice. In wild-type littermates, treatment with rosiglitazone caused a significant decrease in the levels of plasma FFA and triglycerides (Table 1), which was associated with a decrease in adipose tissue lipolysis and an increase in visceral fat content (Fig. 3, A and B). However, in PFKFB3 $^{+/-}$  mice, treatment with rosiglitazone did not bring about significant

## Involvement of iPFK2 in the Effect of PPAR $\gamma$ Activation

changes in any of the above parameters. Additionally, the size of epididymal adipocytes was much larger in rosiglitazone-treated wild-type mice than in rosiglitazone-treated PFKFB3<sup>+/-</sup> mice (Fig. 3C). Together, these data demonstrate that disruption of PFKFB3/iPFK2 lessens the effect of PPAR $\gamma$  activation on increasing adipose tissue fat storage.

**Disruption of PFKFB3/iPFK2 Blunts the Effects of PPAR $\gamma$  Activation on Suppression of HFD-induced Adipose Tissue Inflammatory Response and on Reversal of Adipose Tissue Dysfunction**—Suppression of adipose tissue inflammatory response is one of the major mechanisms by which PPAR $\gamma$  activation reverses insulin resistance and corrects hyperglycemia (6, 21, 46). The effects of PPAR $\gamma$  activation on adipose tissue inflammatory signaling and proinflammatory cytokine expression were determined. In HFD-fed wild-type littermates, treatment with rosiglitazone brought about a decrease in the phosphorylation of JNK1 and NF- $\kappa$ B p65 (Fig. 4, A and B), which was accompanied by a significant decrease in the mRNA levels of TNF $\alpha$  and IL-6 compared with treatment with vehicle (Fig. 4C). Because suppression of adipose tissue inflammatory response is linked to reversal of adipose tissue dysfunction (6, 47), adipose expression of adipokines and insulin signaling were analyzed. Compared with vehicle, treatment with rosiglitazone caused a decrease in adipose mRNA levels of resistin and an increase in adipose mRNA levels of adiponectin (Fig. 4D) and an increase in insulin-stimulated phosphorylation of Akt (Fig. 4E), all of which contributed to the effects of PPAR $\gamma$  activation on reversal of systemic insulin resistance and on correction of hyperglycemia. However, in PFKFB3<sup>+/-</sup> mice, treatment with rosiglitazone did not effectively suppress adipose tissue inflammatory signaling and the mRNA levels of TNF $\alpha$  and IL-6 compared with treatment with vehicle (Fig. 4, A–C). Additionally, treatment with rosiglitazone did not appropriately alter adipose expression of resistin and adiponectin as it did in wild-type mice (Fig. 4D) and failed to increase insulin-stimulated phosphorylation of Akt (Fig. 4E). Collectively, these data demonstrate that disruption of PFKFB3/iPFK2 blunts the effects of PPAR $\gamma$  activation on suppressing HFD-induced adipose inflammatory response and on reversing adipose tissue dysfunction.

**Knockdown of PFKFB3/iPFK2 Lessens the Effect of PPAR $\gamma$  Activation on Stimulating Adipocyte Lipid Accumulation**—The direct role of PFKFB3/iPFK2 in modulating the effect of PPAR $\gamma$  activation on lipid accumulation was explored in iPFK2-KD and iPFK2-Ctrl 3T3-L1 adipocytes. Compared with that in iPFK2-Ctrl cells, the amount of iPFK2 was low and was not increased by rosiglitazone treatment in iPFK2-KD adipocytes (Fig. 5A). Under the basal condition (treatment with vehicle), iPFK2-KD adipocytes accumulated less lipid than did iPFK2-Ctrl adipocytes (Fig. 5, B and C), which was attributed to a decrease in the rate of glucose incorporation into lipid (Fig. 5D). After treatment with rosiglitazone, iPFK2-KD adipocytes exhibited a much smaller increase in lipid accumulation and the rate of glucose incorporation into lipid than did iPFK2-Ctrl adipocytes. This occurred where the response of GyK and PEPCK to PPAR $\gamma$  activation in iPFK2-KD adipocytes was comparable with that in iPFK2-Ctrl adipocytes (supplemental Fig. S2), indicating the importance of PFKFB3/iPFK2 to the

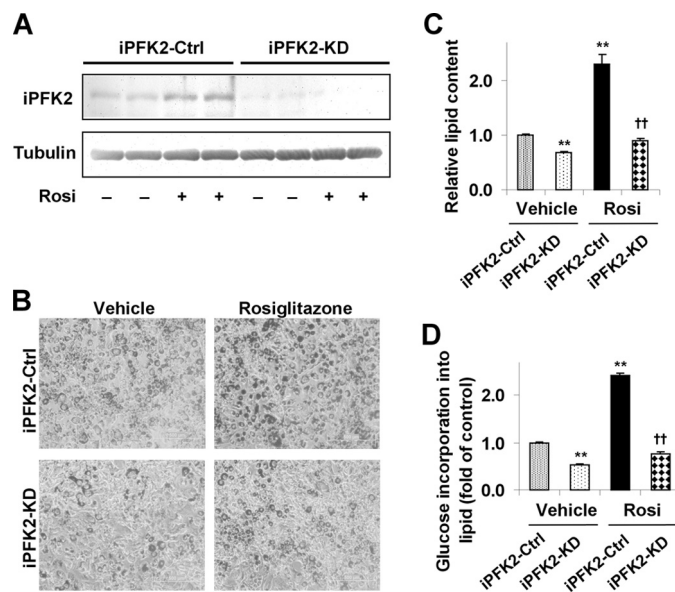


**FIGURE 5. Knockdown of PFKFB3/iPFK2 lessens the effect of PPAR $\gamma$  activation on stimulating adipocyte lipid accumulation.** After differentiation for 6–8 days, stable iPFK2-KD and iPFK2-Ctrl adipocytes were treated with rosiglitazone (Rosi; 1  $\mu$ M) or vehicle (0.1% DMSO) for 48 h. Thereafter, the treated cells were subjected to the assays described under “Experimental Procedures.” *A*, adipocyte iPFK2 was determined using Western blot. *B*, representative images of adipocyte lipid content. Yellow bar, 500  $\mu$ m. For *C* and *D*, data are means  $\pm$  S.E. (error bars),  $n = 4$ . \*\*,  $p < 0.01$ , iPFK2-KD/vehicle or iPFK2-Ctrl/rosiglitazone versus iPFK2-Ctrl/vehicle; ††,  $p < 0.01$ , iPFK2-KD/Rosi versus iPFK2-Ctrl/rosiglitazone. *C*, quantification of adipocyte lipid accumulation (arbitrary units). *D*, changes in the rate of glucose incorporation into lipid.

effect of PPAR $\gamma$  activation on stimulating adipocyte lipid accumulation. These data, consistent with those observed in rosiglitazone-treated PFKFB3<sup>+/-</sup> mice, demonstrate that adipocyte PFKFB3/iPFK2 is needed, at least in part, for PPAR $\gamma$  activation to increase adipose tissue fat storage.

**Knockdown of PFKFB3/iPFK2 Diminishes the Effects of PPAR $\gamma$  Activation on Suppression of Adipocyte Inflammatory Response and on Improvement of Adipocyte Function**—The direct role of PFKFB3/iPFK2 in modulating the effects of PPAR $\gamma$  activation on adipocyte inflammatory response and on adipocyte function was explored. In iPFK2-Ctrl adipocytes, treatment with rosiglitazone caused a significant decrease in palmitate-stimulated phosphorylation of JNK1 and NF- $\kappa$ B p65 (Fig. 6, A and B), which was accompanied by a decrease in the mRNA levels of TNF $\alpha$  and IL-6 (Fig. 6C). In contrast, treatment of iPFK2-KD adipocytes with rosiglitazone did not effectively bring about a significant decrease in palmitate-stimulated phosphorylation of JNK1 and NF- $\kappa$ B p65 and failed to suppress the mRNA levels of TNF $\alpha$  and IL-6 (Fig. 6, A–C). These data, along with those observed in rosiglitazone-treated PFKFB3<sup>+/-</sup> mice, suggest that the intact PFKFB3/iPFK2 in adipocytes is needed, at least in part, for PPAR $\gamma$  activation to suppress adipose tissue inflammatory response.

Increased inflammatory response contributes to inappropriate expression of adipokines and decreased insulin signaling in adipocytes (36). To analyze the direct involvement of PFKFB3/iPFK2 in the effect of PPAR $\gamma$  activation on adipocyte function, the mRNA levels of resistin and adiponectin as well as insulin signaling were determined in rosiglitazone- or vehicle-treated iPFK2-KD and iPFK2-Ctrl adipocytes. Compared with vehicle,

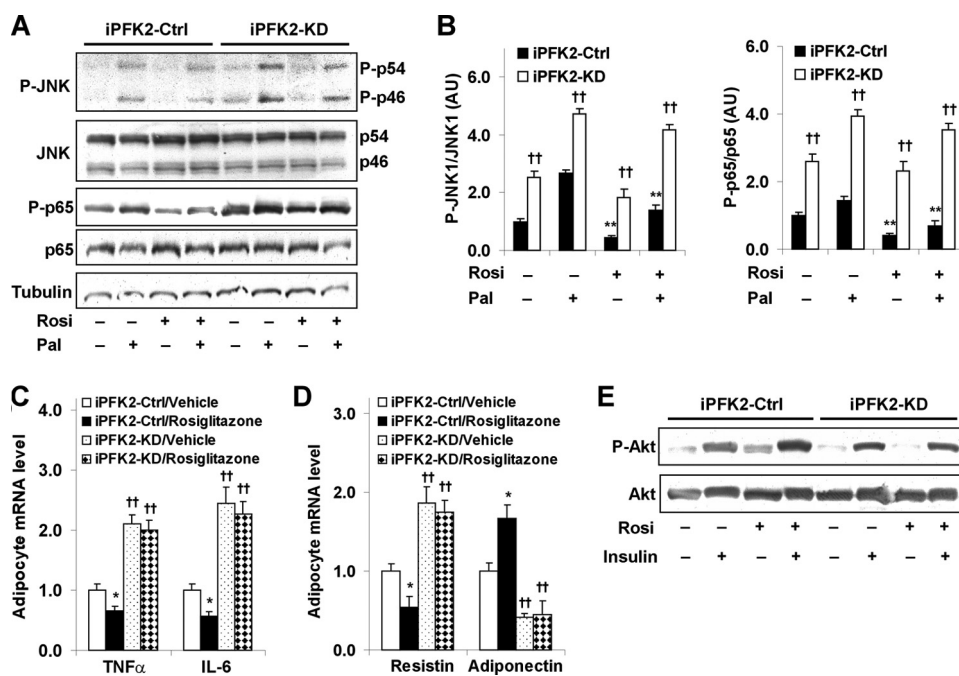


**FIGURE 6. Knockdown of PFKFB3/iPFK2 diminishes the effects of PPAR $\gamma$  activation on both suppression of adipocyte inflammatory response and improvement of adipocyte function.** After differentiation for 6–8 days, stable iPFK2-KD and iPFK2-Ctrl adipocytes were treated with rosiglitazone (Rosi; 1  $\mu$ M) or vehicle (0.1% DMSO) for 48 h in the presence or absence of palmitate (Pal; 250  $\mu$ M) for the last 24 h. Thereafter, the treated cells were subjected to the assays described under "Experimental Procedures." *A*, changes in inflammatory signaling were analyzed using Western blots. For *B–D*, data are means  $\pm$  S.E.,  $n = 4$ . *B*, quantification of inflammatory signaling (arbitrary units). *Left*, phospho-JNK1 (P-JNK1)/JNK1; *right*, phospho-p65 (P-p65)/p65. \*,  $p < 0.01$ , iPFK2-Ctrl treated with Rosi versus iPFK2-Ctrl treated without Rosi in the presence or absence of Pal. ††,  $p < 0.01$ , iPFK2-KD versus iPFK2-Ctrl under the same condition. For *C* and *D*, the expression of proinflammatory cytokines (*C*) and adipokines (*D*) was measured using real-time RT-PCR. \*,  $p < 0.05$ , iPFK2-Ctrl/rosiglitazone versus iPFK2-Ctrl/vehicle for the same gene. ††,  $p < 0.01$ , iPFK2-KD/vehicle versus iPFK2-KD/vehicle or iPFK2-KD/rosiglitazone versus iPFK2-Ctrl/rosiglitazone for the same gene. *E*, adipocyte insulin signaling was analyzed using Western blot. Before harvest, the cells were incubated with or without insulin (100 nM) for 30 min. P-p46, phospho-p46.

treatment with rosiglitazone caused a decrease in the mRNA levels of resistin and an increase in the mRNA levels of adiponectin in iPFK2-Ctrl adipocytes (Fig. 6D). Additionally, treatment with rosiglitazone brought about an increase in insulin-stimulated phosphorylation of Akt in iPFK2-Ctrl adipocytes (Fig. 6E). However, these beneficial effects of rosiglitazone were diminished in iPFK2-KD adipocytes. Together, these data suggest that PFKFB3/iPFK2 is directly involved in the effect of PPAR $\gamma$  activation on improving adipocyte function.

*Inhibition of Fatty Acid Oxidation Restores the Effects of PPAR $\gamma$  Activation on Both Suppression of Adipocyte Inflammatory Response and Stimulation of Adipocyte Insulin Signaling—*PFKFB3/iPFK2 links fuel metabolism and inflammatory response in adipocytes via suppression of fatty acid oxidation-associated production of ROS (36). The extent to which PFKFB3/iPFK2 modulates the effect of PPAR $\gamma$  activation on ROS production was determined. Compared with that in iPFK2-Ctrl adipocytes, the ROS production was higher in iPFK2-KD adipocytes under the basal condition (without palmitate) and was markedly increased in the palmitate-stimulated condition (Fig. 7A). Upon treatment with rosiglitazone, the ROS production was low in iPFK2-Ctrl adipocytes and remained unchanged upon the addition of palmitate. However, in iPFK2-KD adipocytes, rosiglitazone treatment did not significantly decrease the basal ROS production and failed to blunt the palmitate-induced increase in ROS production (Fig. 7A). It appears that PFKFB3/

iPFK2-knockdown-associated increase in ROS production blunts the beneficial effects of PPAR $\gamma$  activation in iPFK2-KD adipocytes. Next, we determined the extent to which correction of excessive ROS production restores the effects of PPAR $\gamma$  activation on inflammatory response and insulin signaling in iPFK2-KD adipocytes. Upon inhibition of fatty acid oxidation by etomoxir, palmitate-stimulated ROS production in iPFK2-KD adipocytes was decreased to a level comparable with that in untreated iPFK2-Ctrl adipocytes (Fig. 7B). Under this condition, treatment with rosiglitazone brought about a decrease in the phosphorylation of JNK1 and NF- $\kappa$ B p65 as well as the mRNA levels of TNF $\alpha$  and IL6 in iPFK2-KD adipocytes to their respective levels comparable with those in rosiglitazone-treated iPFK2-Ctrl adipocytes (Fig. 7, C and D). These effects did not occur in iPFK2-KD adipocytes in the absence of etomoxir (see above; Fig. 6, A–C). Additionally, upon supplementation of etomoxir, treatment with rosiglitazone increased the phosphorylation of Akt in iPFK2-KD adipocytes in the pres-

ence of palmitate (Fig. 7E), which was also not observed in iPFK2-KD adipocytes incubated without etomoxir (see above; Fig. 6E). Collectively, these data suggest that inhibition of excessive fatty acid oxidation restores the effects of PPAR $\gamma$  activation on both suppression of adipocyte inflammatory response and stimulation of adipocyte insulin signaling in iPFK2-KD adipocytes.

## DISCUSSION

PFKFB3/iPFK2 has been identified as a target gene of PPAR $\gamma$  since the finding that troglitazone, an early TZD, increases PFKFB3/iPFK2 expression in adipocytes (33, 34). In the present study, two lines of evidence were obtained to further demonstrate the role of PPAR $\gamma$  in controlling PFKFB3/iPFK2 expression. Notably, disruption of PPAR $\gamma$ 2 decreased PFKFB3/iPFK2 expression, whereas PPAR $\gamma$ 2 overexpression rescued this defect. In addition, agonist(s) for PPAR $\gamma$  but not PPAR $\alpha$  and/or PPAR $\delta$  stimulated the expression of adipocyte PFKFB3/iPFK2, which was attributed to transcription activation of the promoter of PFKFB3. Interestingly, the metabolic phenotype of PFKFB3/iPFK2-disrupted mice (36) was similar to that of PPAR $\gamma$ 2-disrupted mice (40) and adipose tissue-specific PPAR $\gamma$ -knock-out mice on an HFD (12). This leads to the hypothesis that PFKFB3/iPFK2 is critically involved in the anti-diabetic effect of PPAR $\gamma$  activation. To test this hypothesis, using PFKFB3/iPFK2-disrupted mice and PFKFB3/iPFK2-

## Involvement of iPFK2 in the Effect of PPAR $\gamma$ Activation

knockdown 3T3-L1 adipocytes, the present study determined the extent to which PFKFB3/iPFK2 accounts for the anti-diabetic effect of PPAR $\gamma$  activation.

PFKFB3/iPFK2 is involved in the effect of PPAR $\gamma$  activation on increasing adipose tissue fat storage. Notably, rosiglitazone-stimulated adipocyte lipid accumulation, due largely to an

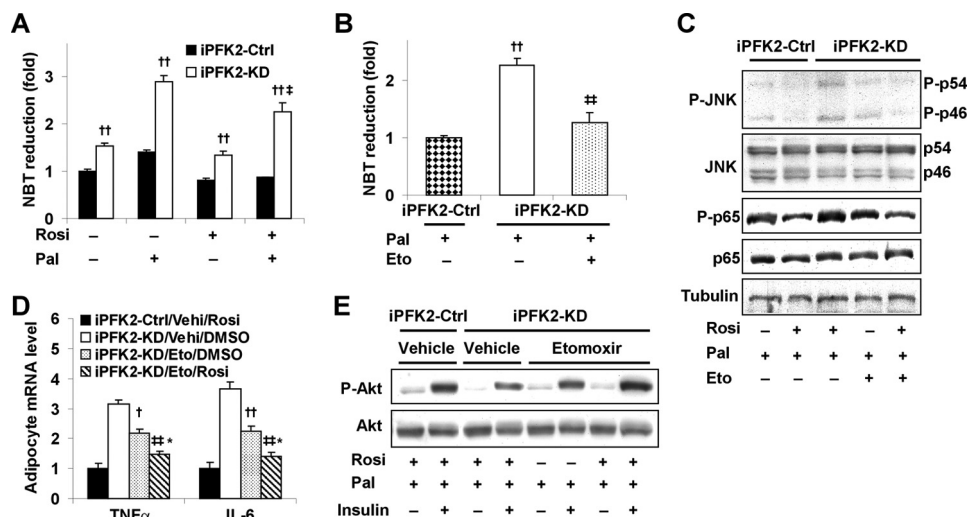


**FIGURE 7. Inhibition of fatty acid oxidation restores the effects of PPAR $\gamma$  activation on both suppression of adipocyte inflammatory response and stimulation of adipocyte insulin signaling.** After differentiation for 6–8 days, stable iPFK2-KD and iPFK2-Ctrl adipocytes were treated with rosiglitazone (*Rosi*; 1  $\mu$ M) or vehicle (0.1% DMSO) for 48 h. In the last 24 h, the cells were incubated with or without etomoxir (*Eto*; 100  $\mu$ M) in the presence or absence of palmitate (*Pal*; 250  $\mu$ M) for 24 h. Thereafter, the treated cells were subjected to the assays described under “Experimental Procedures.” For A and B, the production of ROS was measured using the nitro blue tetrazolium assay. Data are means  $\pm$  S.E. (error bars),  $n = 4$ . A,  $\dagger\dagger$ ,  $p < 0.01$ , iPFK2-KD versus iPFK2-Ctrl under the same condition.  $\ddagger$ ,  $p < 0.05$ , iPFK2-KD in the presence of palmitate versus iPFK2-KD in the absence of palmitate under treatment with rosiglitazone. B,  $\dagger\dagger$ ,  $p < 0.01$  iPFK2-KD versus iPFK2-Ctrl in the absence of etomoxir;  $\ddagger\dagger$ ,  $p < 0.01$  iPFK2-KD in the presence of etomoxir versus iPFK2-KD in the absence of etomoxir. C, changes in adipocyte inflammatory signaling. D, changes in adipocyte expression of proinflammatory cytokines. Data are means  $\pm$  S.E. (error bars),  $n = 4$ .  $\dagger$ ,  $p < 0.05$ ;  $\dagger\dagger$ ,  $p < 0.01$ , iPFK2-KD/etomoxir/DMSO versus iPFK2-KD/vehicle (*Vehi*)/DMSO for the same gene.  $\ddagger\dagger$ ,  $p < 0.01$ , iPFK2-KD/etomoxir/rosiglitazone versus iPFK2-KD/*Vehi*/DMSO; \*,  $p < 0.05$ , iPFK2-KD/etomoxir/rosiglitazone versus iPFK2-KD/etomoxir/DMSO. E, changes in adipocyte insulin signaling. Before harvest, the cells were incubated with or without insulin (100 nM) for 30 min.

increase in glucose incorporation into lipid, is positively correlated with the amount of PFKFB3/iPFK2. In our previous study, we have demonstrated that PFKFB3/iPFK2 increases adipose tissue/adipocyte fat accumulation by stimulation of glycolysis-derived lipogenesis and triglyceride synthesis (36). In the present study, rosiglitazone failed to increase adipose tissue fat storage in PFKFB3 $^{+/-}$  mice, which indicates the importance of PFKFB3/iPFK2 to the effect of PPAR $\gamma$  activation on fat storage. In addition to PFKFB3/iPFK2, GyK and PEPCK are also up-regulated in response to PPAR $\gamma$  activation in adipocytes (16, 24, 25). The role of these two enzymes in participation of PPAR $\gamma$  activation-mediated fat storage has been speculated. In PFKFB3 $^{+/-}$  mice, the response of adipose GyK and PEPCK to rosiglitazone remained intact, suggesting a normal activation of adipose tissue PPAR $\gamma$  in the presence of PFKFB3/iPFK2 disruption. However, the normal response of GyK

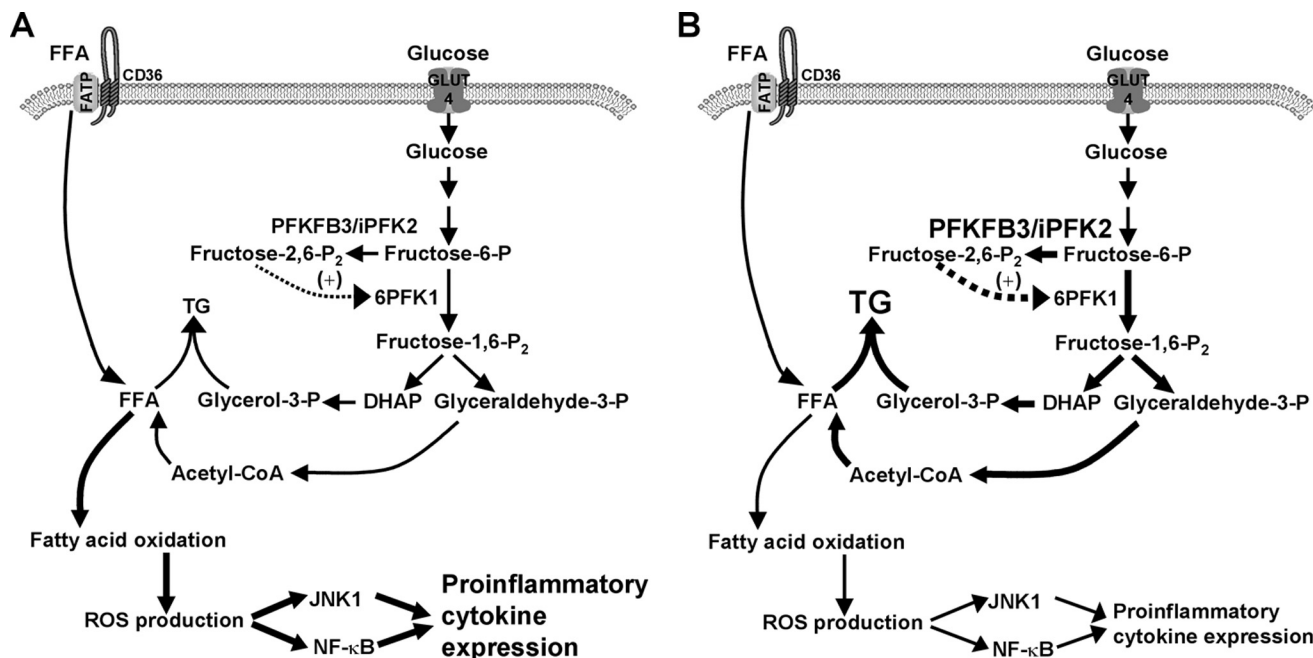


**FIGURE 8. Involvement of PFKFB3/iPFK2 in the effects of PPAR $\gamma$  activation in adipocytes.** Under the condition of overnutrition (A), adipocytes exhibit an increase in inflammatory response, which is brought about at least in part by excessive fatty acid oxidation. Upon activation of PPAR $\gamma$  (B), an increase in the expression of PFKFB3/iPFK2 enhances glycolysis to facilitate the synthesis of triglycerides (TG) via generating glycerol-3-phosphate and FFA (derived from acetyl-CoA following pyruvate oxidation). As a result, an increase in channeling FFA to triglyceride synthesis reduces fatty acid oxidation-associated production of ROS, thereby suppressing inflammatory signaling pathways through JNK1 and NF- $\kappa$ B and decreasing the expression of proinflammatory cytokines. *DHAP*, dihydroxyacetone phosphate; *GLUT4*, glucose transporter 4; *FATP*, fatty acid transport protein.

and PEPCK to rosiglitazone in PFKFB3<sup>+/-</sup> mice was not sufficient to compensate for the PFKFB3/iPFK2 disruption-associated decrease in the ability of adipose tissue to store fat. A possible explanation directly linked to the biochemical properties of these enzymes is that PFKFB3/iPFK2 generates both acetyl-CoA and glycerol 3-phosphate as the required substrates for lipogenesis and triglyceride synthesis in adipocytes (36), whereas GyK and PEPCK appear to only generate glycerol 3-phosphate via direct phosphorylation of glycerol (16) and through glyceroneogenesis (17), respectively. Also, it is possible that the stimulatory effects of GyK and PEPCK on adipocyte/adipose tissue fat storage were offset by the PFKFB3/iPFK2 disruption-associated increase in adipose tissue fatty acid oxidation, given that PFKFB3/iPFK2 has an indirect effect on suppression of adipocyte fatty acid oxidation (36). Based on the current data, the possibility that PFKFB3/iPFK2 disruption generated an environment that could not allow GyK and/or PEPCK to stimulate fat storage cannot be ruled out and will be investigated by future study.

The contribution of PFKFB3/iPFK2 to the anti-diabetic effect of PPAR $\gamma$  activation is also attributable to the suppressive effect of PFKFB3/iPFK2 on adipocyte inflammatory response. Treatment with rosiglitazone brought about a decrease in HFD-stimulated adipose mRNA levels of TNF $\alpha$  and IL-6 in wild-type mice but not in PFKFB3<sup>+/-</sup> mice. Further, a direct role for PFKFB3/iPFK2 in mediating the anti-inflammatory effect of PPAR $\gamma$  activation was confirmed in a cell culture system. In PFKFB3/iPFK2-knockdown 3T3-L1 adipocytes, rosiglitazone did not decrease palmitate-induced mRNA levels of TNF $\alpha$  and IL-6 as it did in control adipocytes. This PFKFB3/iPFK2-knockdown-associated defect resulted in an inefficiency of rosiglitazone to decrease adipose resistin mRNA levels and to increase adiponectin mRNA levels in both PFKFB3<sup>+/-</sup> mice and PFKFB3/iPFK2-knockdown adipocytes, which indicated adipose tissue/adipocyte dysfunction (47–49) and contributed to the lack of anti-diabetic effect in rosiglitazone-treated PFKFB3<sup>+/-</sup> mice.

In the adipose tissue, both macrophages and adipocytes are key determinants of overnutrition-induced adipose tissue inflammatory response (50–53). Attention has been increasingly paid to the effect of PPAR $\gamma$  activation on suppression of the proinflammatory function of macrophages (21, 54, 55). Considering the importance of adipocyte PPAR $\gamma$  activation to whole-body insulin sensitivity (8), the present study focused on the effect of PPAR $\gamma$  activation on adipocyte inflammatory response. We observed that treatment with rosiglitazone effectively reduced the phosphorylation of JNK1 and NF- $\kappa$ B p65 in control adipocytes but not in PFKFB3/iPFK2-knockdown adipocytes. This is consistent with the observation that rosiglitazone blunted palmitate-induced ROS production in control adipocytes but not in PFKFB3/iPFK2-knockdown adipocytes. When PFKFB3/iPFK2 disruption-associated excessive fatty acid oxidation was brought down with etomoxir treatment, rosiglitazone was able to decrease inflammatory response and stimulate insulin signaling in PFKFB3/iPFK2-knockdown adipocytes. Clearly, PFKFB3/iPFK2 contributes to the anti-inflammatory effect of PPAR $\gamma$  activation through a mechanism

involving suppression of excessive fatty acid oxidation in adipocytes.

In conclusion, the present study provides data to support the involvement of PFKFB3/iPFK2 in the anti-diabetic effect of PPAR $\gamma$  activation. This role of PFKFB3/iPFK2 is evidenced by the fact that the intact PFKFB3/iPFK2 allows rosiglitazone to increase fat storage in the adipocytes/adipose tissue and to suppress adipocyte/adipose tissue inflammatory response. Mechanistically, the way by which PFKFB3/iPFK2 links two adipose tissue-based mechanisms underlying the anti-diabetic effect of PPAR $\gamma$  activation is attributable to the effect of PFKFB3/iPFK2 on regulating adipocyte lipogenesis and triglyceride synthesis as well as adipocyte fatty acid oxidation-related ROS production and inflammatory response (Fig. 8). These results indicate that selective activation of adipocyte PFKFB3/iPFK2 may be a viable approach to generating the beneficial effects of PPAR $\gamma$  activation in the treatment of type 2 diabetes.

## REFERENCES

- Lehmann, J. M., Moore, L. B., Smith-Oliver, T. A., Wilkison, W. O., Willson, T. M., and Kliewer, S. A. (1995) *J. Biol. Chem.* **270**, 12953–12956
- Berger, J., Bailey, P., Biswas, C., Cullinan, C. A., Doebber, T. W., Hayes, N. S., Saperstein, R., Smith, R. G., and Leibowitz, M. D. (1996) *Endocrinology* **137**, 4189–4195
- Lebovitz, H. E., Dole, J. F., Patwardhan, R., Rappaport, E. B., and Freed, M. I. (2001) *J. Clin. Endocrinol. Metab.* **86**, 280–288
- Phillips, L. S., Grunberger, G., Miller, E., Patwardhan, R., Rappaport, E. B., and Salzman, A. (2001) *Diabetes Care* **24**, 308–315
- Krentz, A. J., Bailey, C. J., and Melander, A. (2000) *BMJ* **321**, 252–253
- Evans, R. M., Barish, G. D., and Wang, Y. X. (2004) *Nat. Med.* **10**, 355–361
- Grundy, S. M. (2006) *Nat. Rev. Drug Discov.* **5**, 295–309
- Sugii, S., Olson, P., Sears, D. D., Saberi, M., Atkins, A. R., Barish, G. D., Hong, S. H., Castro, G. L., Yin, Y. Q., Nelson, M. C., Hsiao, G., Greaves, D. R., Downes, M., Yu, R. T., Olefsky, J. M., and Evans, R. M. (2009) *Proc. Natl. Acad. Sci. U.S.A.* **106**, 22504–22509
- Matsusue, K., Haluzik, M., Lambert, G., Yim, S. H., Gavrilo, O., Ward, J. M., Brewer, B., Jr., Reitman, M. L., and Gonzalez, F. J. (2003) *J. Clin. Invest.* **111**, 737–747
- Norris, A. W., Chen, L., Fisher, S. J., Szanto, I., Ristow, M., Jozsi, A. C., Hirshman, M. F., Rosen, E. D., Goodyear, L. J., Gonzalez, F. J., Spiegelman, B. M., and Kahn, C. R. (2003) *J. Clin. Invest.* **112**, 608–618
- Chao, L., Marcus-Samuels, B., Mason, M. M., Moitra, J., Vinson, C., Arioglu, E., Gavrilo, O., and Reitman, M. L. (2000) *J. Clin. Invest.* **106**, 1221–1228
- He, W., Barak, Y., Hevener, A., Olson, P., Liao, D., Le, J., Nelson, M., Ong, E., Olefsky, J. M., and Evans, R. M. (2003) *Proc. Natl. Acad. Sci. U.S.A.* **100**, 15712–15717
- Kintscher, U., and Law, R. E. (2005) *Am. J. Physiol. Endocrinol. Metab.* **288**, E287–E291
- Lehrke, M., and Lazar, M. A. (2005) *Cell* **123**, 993–999
- Qatanani, M., and Lazar, M. A. (2007) *Genes Dev.* **21**, 1443–1455
- Guan, H. P., Li, Y., Jensen, M. V., Newgard, C. B., Steppan, C. M., and Lazar, M. A. (2002) *Nat. Med.* **8**, 1122–1128
- Leroyer, S. N., Tordjman, J., Chauvet, G., Quette, J., Chapron, C., Forest, C., and Antoine, B. (2006) *J. Biol. Chem.* **281**, 13141–13149
- Kolak, M., Yki-Järvinen, H., Kannisto, K., Tiikkainen, M., Hamsten, A., Eriksson, P., and Fisher, R. M. (2007) *J. Clin. Endocrinol. Metab.* **92**, 720–724
- Kershaw, E. E., Schupp, M., Guan, H. P., Gardner, N. P., Lazar, M. A., and Flier, J. S. (2007) *Am. J. Physiol. Endocrinol. Metab.* **293**, E1736–E1745
- Wellen, K. E., Uysal, K. T., Wiesbrock, S., Yang, Q., Chen, H., and Hotamisligil, G. S. (2004) *Endocrinology* **145**, 2214–2220
- Stienstra, R., Duval, C., Keshtkar, S., van der Laak, J., Kersten, S., and Müller, M. (2008) *J. Biol. Chem.* **283**, 22620–22627
- Combs, T. P., Wagner, J. A., Berger, J., Doebber, T., Wang, W. J., Zhang,

## Involvement of *i*PFK2 in the Effect of PPAR $\gamma$ Activation

- B. B., Tanen, M., Berg, A. H., O'Rahilly, S., Savage, D. B., Chatterjee, K., Weiss, S., Larson, P. J., Gottesdiener, K. M., Gertz, B. J., Charron, M. J., Scherer, P. E., and Moller, D. E. (2002) *Endocrinology* **143**, 998–1007
23. Tontonoz, P., and Spiegelman, B. M. (2008) *Annu. Rev. Biochem.* **77**, 289–312
24. Tontonoz, P., Hu, E., Devine, J., Beale, E. G., and Spiegelman, B. M. (1995) *Mol. Cell Biol.* **15**, 351–357
25. Devine, J. H., Eubank, D. W., Clouthier, D. E., Tontonoz, P., Spiegelman, B. M., Hammer, R. E., and Beale, E. G. (1999) *J. Biol. Chem.* **274**, 13604–13612
26. Ranganathan, G., Unal, R., Pokrovskaya, I., Yao-Borengasser, A., Phananvanh, B., Lecka-Czernik, B., Rasouli, N., and Kern, P. A. (2006) *J. Lipid Res.* **47**, 2444–2450
27. Duplus, E., Benelli, C., Reis, A. F., Fouque, F., Velho, G., and Forest, C. (2003) *Biochimie* **85**, 1257–1264
28. Forest, C., Tordjman, J., Glorian, M., Duplus, E., Chauvet, G., Quette, J., Beale, E. G., and Antoine, B. (2003) *Biochem. Soc. Trans.* **31**, 1125–1129
29. Tan, G. D., Debard, C., Tiraby, C., Humphreys, S. M., Frayn, K. N., Langin, D., Vidal, H., and Karpe, F. (2003) *Nat. Med.* **9**, 811–812
30. Franckhauser, S., Muñoz, S., Elias, I., Ferre, T., and Bosch, F. (2006) *Diabetes* **55**, 273–280
31. Xu, H., Barnes, G. T., Yang, Q., Tan, G., Yang, D., Chou, C. J., Sole, J., Nichols, A., Ross, J. S., Tartaglia, L. A., and Chen, H. (2003) *J. Clin. Invest.* **112**, 1821–1830
32. Permana, P. A., Zhang, W., Wabitsch, M., Fischer-Posovszky, P., Duckworth, W. C., and Reaven, P. D. (2009) *Am. J. Physiol. Endocrinol. Metab.* **296**, E1076–E1084
33. Nielsen, R., Pedersen, T. A., Hagenbeek, D., Moulos, P., Siersbaek, R., Megens, E., Denissov, S., Borgesen, M., Francoijs, K. J., Mandrup, S., and Stunnenberg, H. G. (2008) *Genes Dev.* **22**, 2953–2967
34. Atsumi, T., Nishio, T., Niwa, H., Takeuchi, J., Bando, H., Shimizu, C., Yoshioka, N., Bucala, R., and Koike, T. (2005) *Diabetes* **54**, 3349–3357
35. Chesney, J., Telang, S., Yalcin, A., Clem, A., Wallis, N., and Bucala, R. (2005) *Biochem. Biophys. Res. Commun.* **331**, 139–146
36. Huo, Y., Guo, X., Li, H., Wang, H., Zhang, W., Wang, Y., Zhou, H., Gao, Z., Telang, S., Chesney, J., Chen, Y. E., Ye, J., Chapkin, R. S., and Wu, C. (2010) *J. Biol. Chem.* **285**, 3713–3721
37. Wu, C., Okar, D. A., Newgard, C. B., and Lange, A. J. (2001) *J. Clin. Invest.* **107**, 91–98
38. Wu, C., Kang, J. E., Peng, L. J., Li, H., Khan, S. A., Hillard, C. J., Okar, D. A., and Lange, A. J. (2005) *Cell Metabolism* **2**, 131–140
39. Wu, C., Khan, S. A., Peng, L. J., Li, H., Carmella, S. G., and Lange, A. J. (2006) *Am. J. Physiol. Endocrinol. Metab.* **291**, E536–E543
40. Zhang, J., Fu, M., Cui, T., Xiong, C., Xu, K., Zhong, W., Xiao, Y., Floyd, D., Liang, J., Li, E., Song, Q., and Chen, Y. E. (2004) *Proc. Natl. Acad. Sci. U.S.A.* **101**, 10703–10708
41. Berger, J. J., and Barnard, R. J. (1999) *J. Appl. Physiol.* **87**, 227–232
42. Haemmerle, G., Zimmermann, R., Hayn, M., Theussl, C., Waeg, G., Wagner, E., Sattler, W., Magin, T. M., Wagner, E. F., and Zechner, R. (2002) *J. Biol. Chem.* **277**, 4806–4815
43. Cao, H., Gerhold, K., Mayers, J. R., Wiest, M. M., Watkins, S. M., and Hotamisligil, G. S. (2008) *Cell* **134**, 933–944
44. Stansbie, D., Brownsey, R. W., Crettaz, M., and Denton, R. M. (1976) *Biochem. J.* **160**, 413–416
45. Subauste, A. R., and Burant, C. F. (2007) *Am. J. Physiol. Endocrinol. Metab.* **293**, E159–E164
46. Díaz-Delfín, J., Morales, M., and Caelles, C. (2007) *Diabetes* **56**, 1865–1871
47. Guilherme, A., Virbasius, J. V., Puri, V., and Czech, M. P. (2008) *Nat. Rev. Mol. Cell Biol.* **9**, 367–377
48. Greenberg, A. S., and Obin, M. S. (2006) *Am. J. Clin. Nutr.* **83**, 461S–465S
49. Trujillo, M. E., and Scherer, P. E. (2006) *Endocr. Rev.* **27**, 762–778
50. Weisberg, S. P., McCann, D., Desai, M., Rosenbaum, M., Leibel, R. L., and Ferrante, A. W., Jr. (2003) *J. Clin. Invest.* **112**, 1796–1808
51. Kamei, N., Tobe, K., Suzuki, R., Ohsugi, M., Watanabe, T., Kubota, N., Ohtsuka-Kawatari, N., Kumagai, K., Sakamoto, K., Kobayashi, M., Yamachi, T., Ueki, K., Oishi, Y., Nishimura, S., Manabe, I., Hashimoto, H., Ohnishi, Y., Ogata, H., Tokuyama, K., Tsunoda, M., Ide, T., Murakami, K., Nagai, R., and Kadowaki, T. (2006) *J. Biol. Chem.* **281**, 26602–26614
52. Lumeng, C. N., Bodzin, J. L., and Saltiel, A. R. (2007) *J. Clin. Invest.* **117**, 175–184
53. Lumeng, C. N., Deyoung, S. M., Bodzin, J. L., and Saltiel, A. R. (2007) *Diabetes* **56**, 16–23
54. Bouhrel, M. A., Derudas, B., Rigamonti, E., Dièvert, R., Brozek, J., Haulon, S., Zawadzki, C., Jude, B., Torpier, G., Marx, N., Staels, B., and Chinetti-Gbaguidi, G. (2007) *Cell Metabolism* **6**, 137–143
55. Fujisaka, S., Usui, I., Bukhari, A., Ikutani, M., Oya, T., Kanatani, Y., Tsuneyama, K., Nagai, Y., Takatsu, K., Urakaze, M., Kobayashi, M., and Tobe, K. (2009) *Diabetes* **58**, 2574–2582